12.4 INTRUSION INTO A DENSITY-STRATIFIED CROSSFLOW – A MODEL FOR SPREADING VOLCANIC ASH CLOUD

Peter G Baines*
Dept. of Infrastructure Engineering, University of Melbourne
Melbourne, Australia

1. INTRODUCTION

The atmospheric flow that results from a volcanic eruption typically consists of a rising plume of a mixture of hot rock fragments and heated air. This mixture reaches a level of neutral buoyancy in the upper troposphere or stratosphere, where it spreads laterally. Some eruptions have an explosive nature and are of short duration (of 1-2 minutes), such as those on the Caribbean island of Montserrat. Others continue for an extended period at an approximately uniform rate of emission, such as the recent eruption of Puyehue in Chile (see Figure 1), and various recent eruptions in Iceland such as those of Eyjafjallajökul in 2010.

Each sufficiently large ash cloud leaves a deposit of sediment on the surface when the particulate material falls out of the cloud, and the neighbourhoods of significant volcanic sites are notably marked with layers of such sediment as a record of past eruptions. In this paper, I consider the nature and shape of such ash clouds, modelled as spreading intrusions from a steady source at an elevated level, in stratified environments with and without a crosswind. Although ash cloud dynamics was the motivating factor, this study addresses the general question of the dynamics of such intrusions. Other applications are possible, such as flow from deep cumulonimbus, sewage outfalls in stratified coastal environments, and flows from deep sources in, for example, the Gulf of Mexico. Studies of this type of flow from an engineering perspective have been made by G.H. Jirka, and a survey of the results obtained are described in Akar & Jirka (1995a, b).

In the present study, the objective is to obtain a physical and dynamical description of flow from a finite source region in a density-stratified environment without, in the first instance, invoking frictional and mixing processes as an essential part of the dynamical balance (though clearly they may be added later if appropriate). The most important of these processes – the drag on the intrusion due to its motion relative to the environment – is included in the analysis where it is important, namely in the far field, at large distances from the source.

The flows described here depend on 3 parameters: Q, the volume flux from the source, N, the buoyancy frequency of the environment, and u_e, the relative velocity of the environmental fluid. The relevant dimensionless parameter governing these flows is then $u_e/(QN^2)^{1/3}$, which is contained in the parameter ε, defined below.

2. DYNAMICAL MODEL AND BASIC EQUATIONS

The model used here is essentially the same as that described in Baines et al. (2008), with the difference that the source is maintained at a steady rate and the background environment is moving at a uniform speed relative to the source. We assume that the intrusive fluid is produced from a source at lower (ground) levels, and rises as a buoyant plume to a level of neutral density, where it spreads. We are (mostly) here concerned with the manner of the spreading of this fluid in the presence of a crossflow, and assume that the fluid is homogeneous, incompressible and effectively inviscid, at least in the vicinity of the source.

For an intrusion layer of thickness d and density , the hydrostatic pressure is

$$p = p_c(0) - \rho_0 gz + \frac{1}{8}\rho_0 N^2 d^2, \quad N^2 = -\frac{g}{\rho}\frac{\mathrm{d}\rho}{\mathrm{dz}}, \qquad (1)$$

where N is the buoyancy frequency. The principal governing equations are then

$$\frac{\partial \boldsymbol{u}}{\partial \boldsymbol{t}} + \boldsymbol{u}.\nabla\boldsymbol{u} = -\frac{1}{\rho_0}\nabla p = -\frac{N^2}{8}\nabla d^2, \qquad (2)$$

$$\frac{\partial d}{\partial t} + \nabla.(d\boldsymbol{u}) = 0, \quad \nabla x\boldsymbol{u} = 0.$$

These represent the momentum equation, conservation of mass/volume, and irrotational flow, the latter condition applying because all

---

* *Corresponding author address*: Peter G Baines, Dept. of Infrastructure Engineering, University of Melbourne, Grattan Street, Melbourne, VIC 3010 Australia . email: p.baines@unimelb.edu.au

the fluid in the intrusion has come from a localised source. Assuming steady-state flow, the first of equations (2) may be integrated to give the Bernoulli equation

$$\boldsymbol{u}^2 + \left(\frac{Nd}{2}\right)^2 = C^2, \quad (3)$$

where C is a constant. If we also assume that the flow is in a steady crosswind of speed u_e, this becomes (Milne-Thomson 1960)

$$\boldsymbol{u}^2 + \left(\frac{Nd}{2}\right)^2 = C^2 + u_e^2. \quad (4)$$

A rising plume of fluid provides a localised source of fluid to the intrusive layer, and this may be modelled by a constant source of homogeneous fluid at the neutral level, spreading radially at a uniform rate in all directions within a radius r_s, which defines the spatial size of this source region. Accordingly, at the radius r_s we have

$$2\pi r_s d_s u_s = Q, \quad (5)$$

where Q denotes the volume flux of the source, and d_s, u_s the thickness and radial velocity of the intrusive fluid at $r = r_s$. r_s depends on plume dynamics, and may be expressed as

$$r_s = a_s\left(\frac{Q}{N}\right)^{1/3}, \quad (6)$$

where a_s is of order unity.

For $r < r_s$ the flow is dominated by the dynamics of the plume, with negligible influence of the external flow, whereas for $r > r_s$ the effect of the external flow is significant. The parameter C may be defined in terms of Q and N by the relation

$$C = \left(\frac{QN}{2\pi r_s}\right)^{1/2} = \frac{\left(QN^2\right)^{1/3}}{\left(2\pi a_s\right)^{1/2}}. \quad (7)$$

In the absence of any external flow, taking r_s to be the minimum possible value of r, for steady flow (4) and (5) imply that

$$u_s = \frac{Nd_s}{2}, \quad (8)$$

with $$d_s = \left(\frac{1}{a_s\pi}\right)^{1/2}\left(\frac{Q}{N}\right)^{1/3}. \quad (9)$$

Hence $d_s < r_s$, if $a_s \geq 1$.We next non-dimensionalise the variables by the constant C, so that

$\boldsymbol{U} = \boldsymbol{u}/C$, $D=Nd/2C$, $\varepsilon = u_e/C$, (10)

and the equations governing the steady-state flow inside the intrusion are then

$$\boldsymbol{U}^2 + D^2 - 1 - \varepsilon^2 = 0, \quad (11)$$

$$\nabla x\boldsymbol{U} = 0, \quad \nabla.(D\boldsymbol{U}) = 0. \quad (12)$$

These equations constitute an hydraulic system that is analogous to that for a single layer of fluid with a free surface. Flows may be classified as sub- (D > |$\boldsymbol{U}$|) or super-critical (D<|$\boldsymbol{U}$|), implying that waves may or may not be able to propagate upsteam against the mean flow of the layer. They must be then solved numerically, but, as with single-layer flows, the degree of criticality must be considered in the interpretation of flow solutions. For situations of interest, ε is in the range $0 < \varepsilon < 1$.

Figure 1. An aerial view shows ash and steam from an eruption in the Puyehue-Cordon Caulle volcanic chain near Osorno city in south-central Chile, on June 5, 2011. Picture taken through a plane window. (Reuters/Ivan Alvarado).

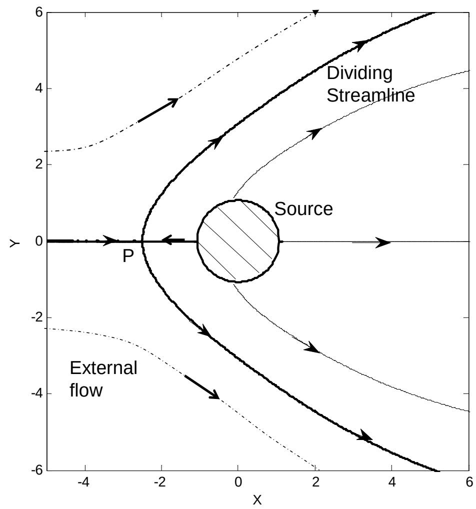

Figure 2. Schematic diagram of the horizontal pattern of flow within and around the intrusion. P denotes the upstream stagnation point, and dot-dashed lines denote flow outside the intrusion.

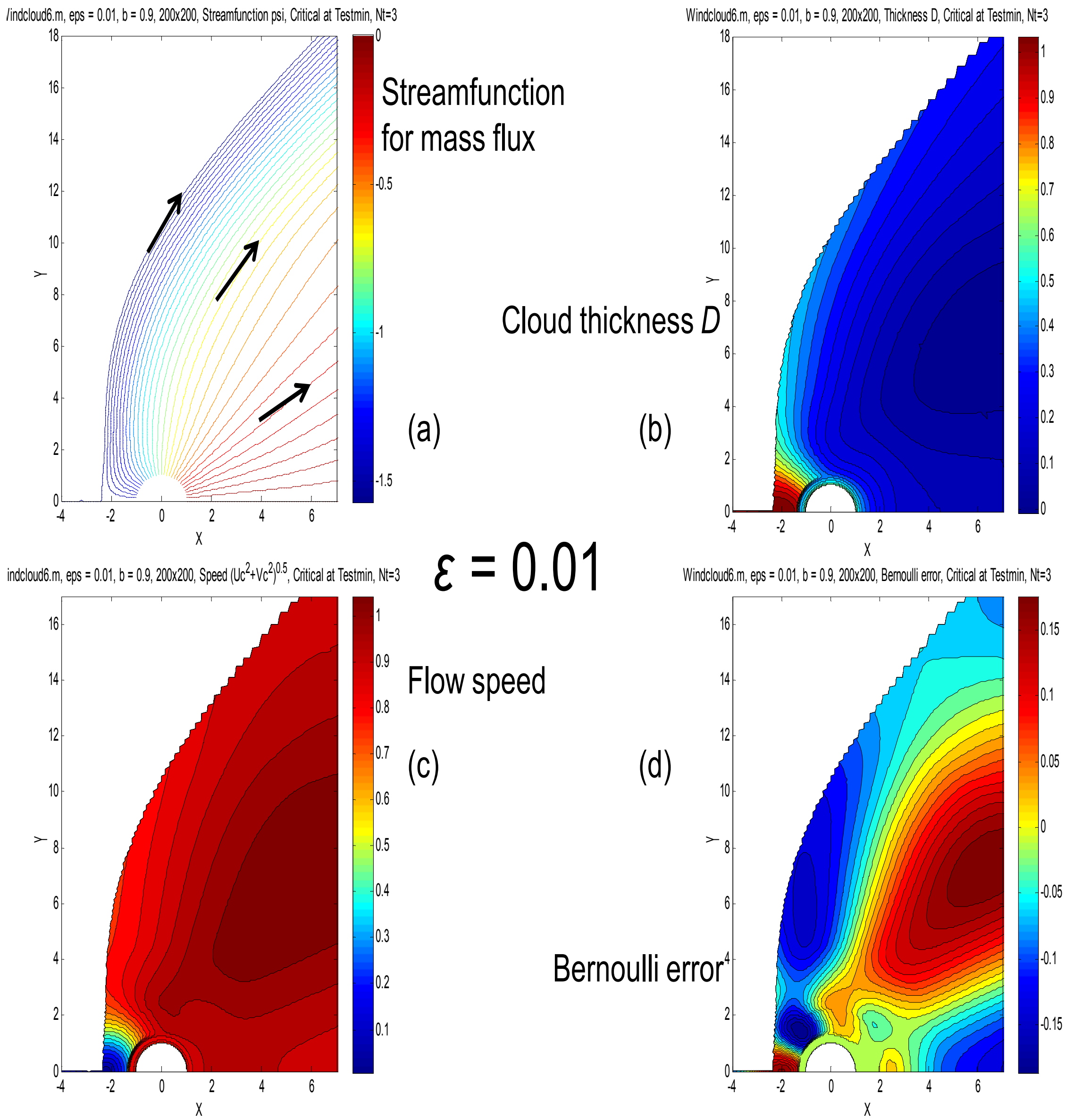

Figure 3. The transcritical flow solution in the neighbourhood of the source for ε = 0.01. Frame (a) shows the stream function for the mass/volume flux; frame (b) shows the thickness *D*; frame (c) shows the fluid speed, directed along the contours in frame (a), and frame (d) shows the degree of satisfaction of the Bernoulli equation, which is an estimate of the error in the solution. All contours are equally spaced in the values of their respective variables.

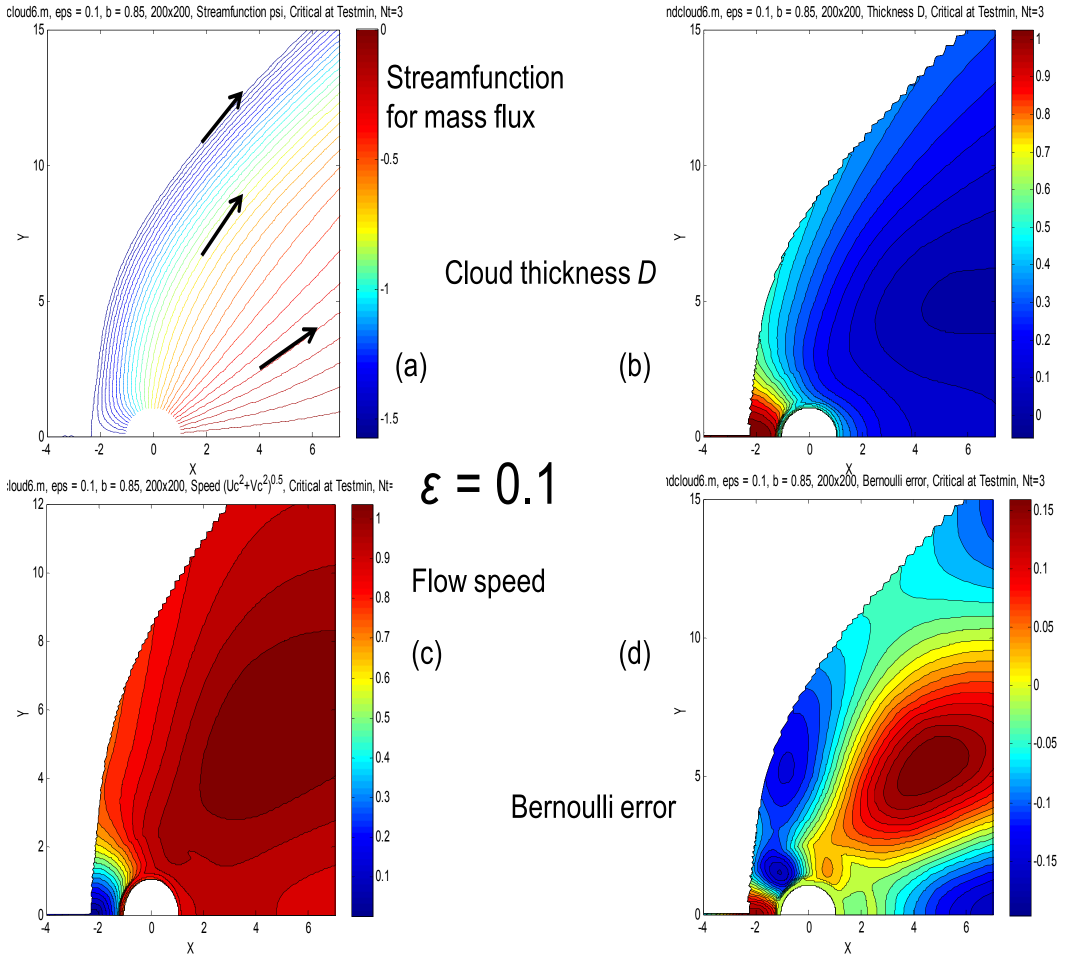

Figure 4. As for Figure 3, but for ε = 0.1.

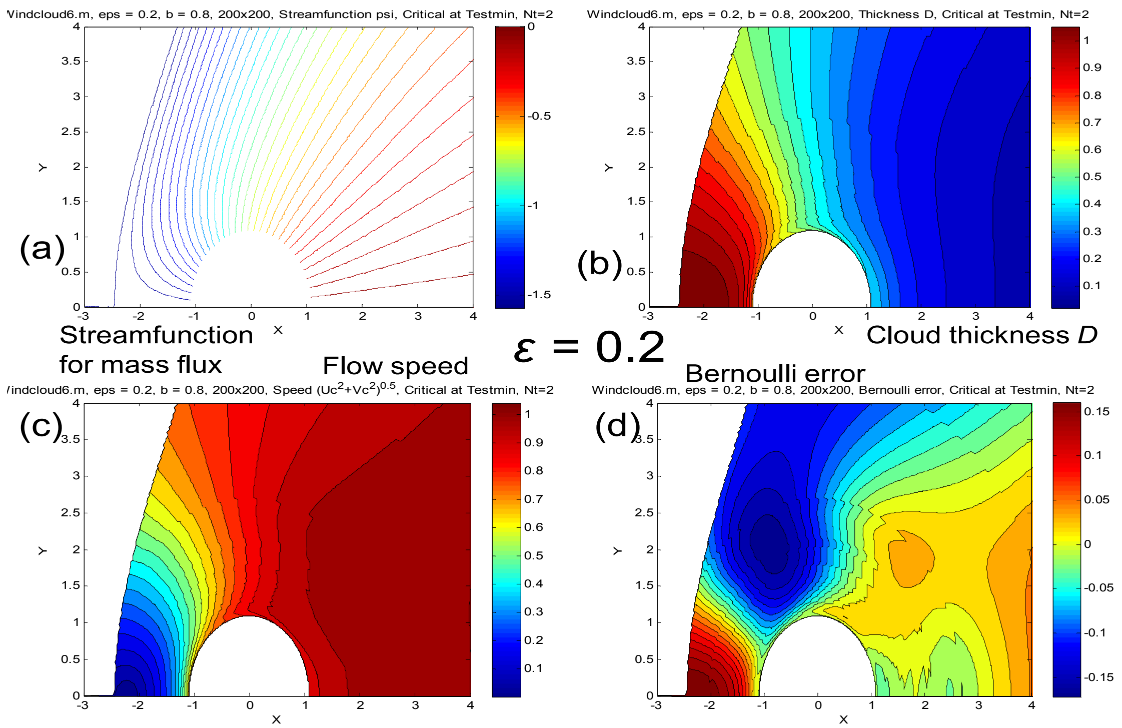

Figure 5. As for Figure 3, but for ε = 0.2.

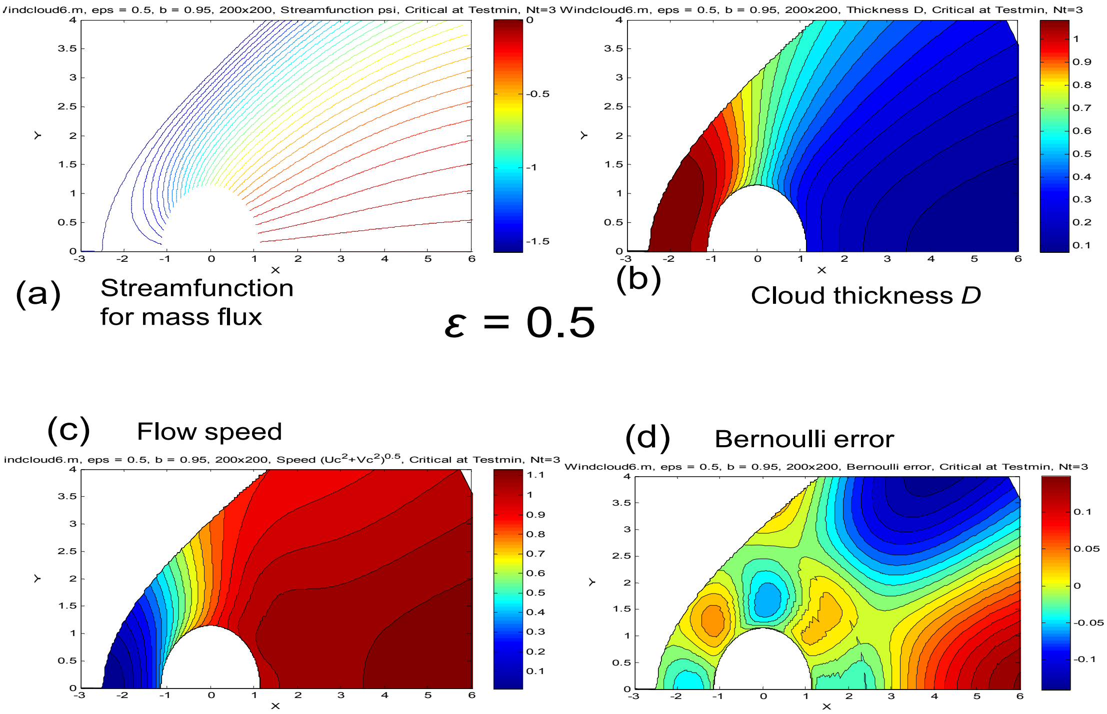

Figure 6. As for Figure 3, but for ε = 0.5.

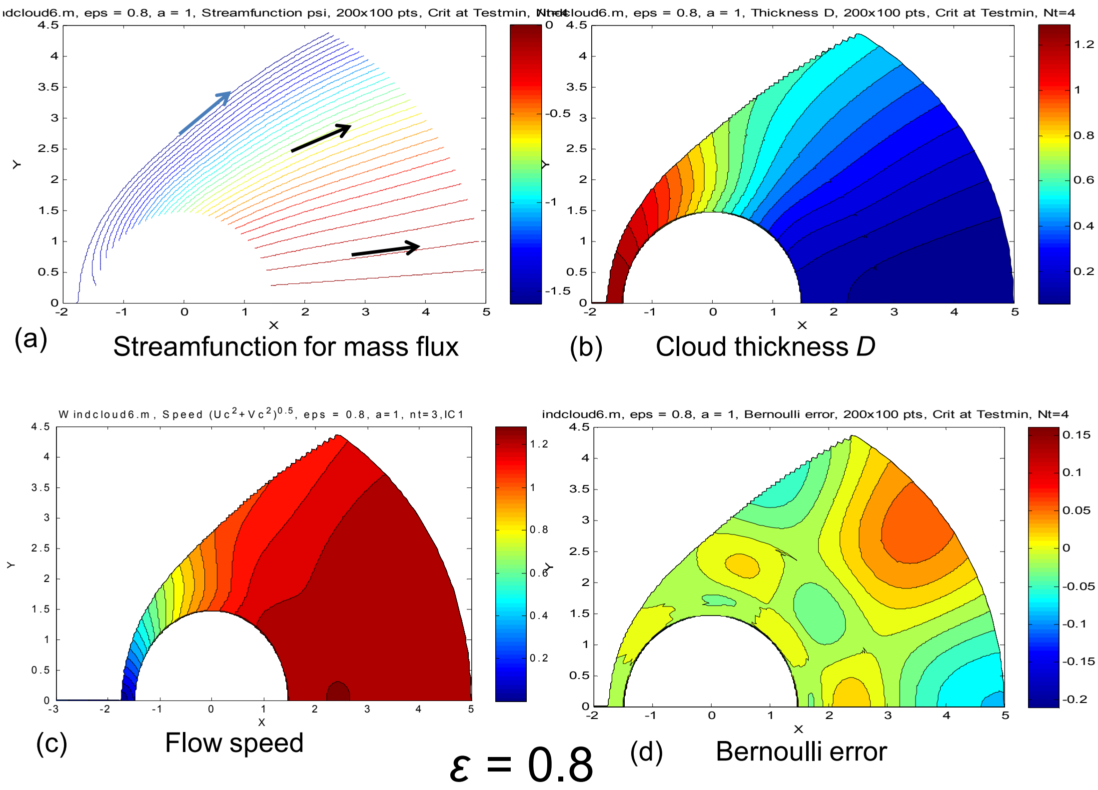

Figure 7. As for Figure 3, but for ε = 0.8.

3. FLOW WITHOUT AMBIENT WIND

Without an ambient background wind, the intrusive flow is axi-symmetric, $\varepsilon = 0$, and (5) applies to all radii with $R = r/r_s > 1$, in the form

$$DU=1/2R. \qquad (13)$$

Axisymmetric solutions to (11-12) then give

$$D^2 = \frac{1}{2} - \frac{1}{2}\left(1 - \frac{1}{R^2}\right)^{1/2}, \quad U^2 = \frac{1}{2} + \frac{1}{2}\left(1 - \frac{1}{R^2}\right)^{1/2} \qquad (14)$$

The intrusion spreads like a pancake, with

$$U \sim 1, \text{ and } D \sim 1/2R., \text{ for } R \to \infty . \qquad (15)$$

4. FLOW SOLUTIONS NEAR THE SOURCE IN CROSSWIND

The nature of the flow in plan view is shown in Figure 2. In general, the flow pattern within the intrusion is two-dimensional, whereas the external flow of the *stratified* environment is three-dimensional. However, the intrusion necessarily has an upstream stagnation point P, and from the Bernoulli equation this implies that the thickness D is a maximum there, with the value $(1+\varepsilon^2)^{1/2} > 1$. This implies that the quantity $D/\varepsilon > 1$ also. If one regards the ash cloud as an obstacle within the environmental flow field, D/ε is equal to the quantity "Nh/U" applying to stratified flow of speed U past topography of height h. If $Nh/U > 1$, the flow is primarily around the obstacle, rather than over it (Baines 1995), and this is certainly the case for volcanic ash clouds in the parameter range of interest Further, the blocking process causes the external stratification to weaken at the levels of the intrusion, so that the density there is approximately that of the fluid inside the cloud.

In consequence, the flow near the source region is approximately two-dimensional both inside and outside the cloud, and the above equations (11, 12) are expected to have some validity beyond the distance of the separation point.

The numerical procedure involves a low-order Fourier expansion around the source. Assuming simple conditions at the source that are consistent with equations (11,12) and represent a simple source in a crossflow, one may obtain solutions that describe the flow in the neighbourhood of the source (the details of how this is done will be described elsewhere). Two types of solution are obtained. The first type consists of flow that is everywhere subcritical near the source, but this is unrealistic because it cannot be matched with a far-field flow that must be supercritical as it expands and thins. The second type of flow is "transcritical", in that the flow is subcritical near the upstream stagnation point, but becomes supercritical as it passes around the source. These solutions are therefore quite realistic, and examples for a range of values of ε are shown in Figures 3-7.

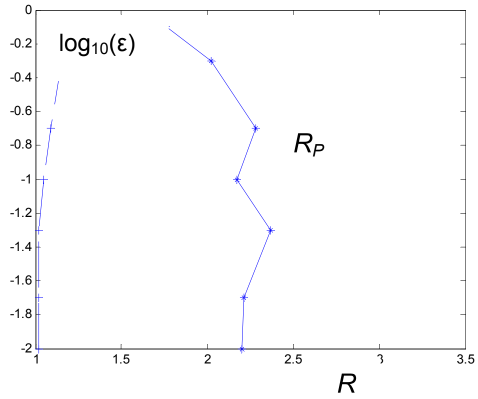

Figure 8. Dependence of the position of the upstream stagnation point on ε.

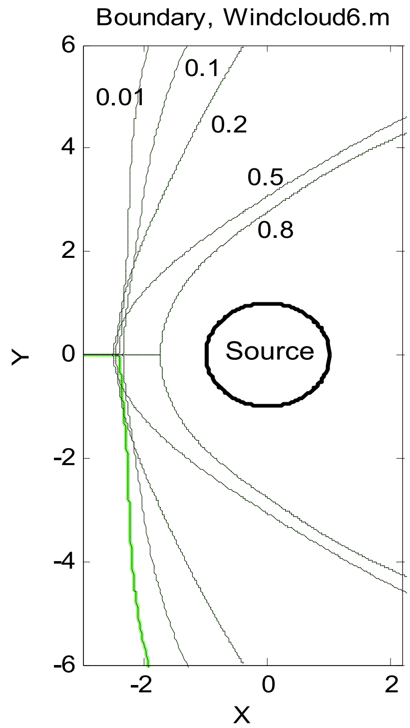

Figure 9. Positions of the upstream boundary of the intrusion as a function of parameter ε, in plan view, the latter representing the relative upstream crosswind speed.

In all of these figures, the mass/volume flux (as interpreted from the spacing of the contours in Figures 3-7(a)) is largest near the boundary of the cloud. For small ε, the region of thick, subcritical intrusion ($D > 0.7$) is confined to a lateral distance of order r_s in front of the source (near θ = 180°), but as ε increases above 0.1 it expands around the source to $\theta \approx 90°$. In all cases, D is a minimum on the centreline, the positive X-axis. The flow speed is a maximum there for $\varepsilon \geq 0.5$, but as ε decreases it moves off-axis to $\theta \sim 45°$ for $\varepsilon << 1$. The "Bernoulli error" represents the sum of the terms in the Bernoulli equation, which should sum to zero. Individual terms have maximum value ~ 1, so that values less than 0.05 represent 5% error, etc.. The errors are smallest for ε = 0.8, and tend to become larger for increasing R. They are generally less than 10% for R < 3.

Perhaps the most remarkable property of these flow solutions is the dependence of R_P on ε, shown in Figure 8. It is clear that the position of R_P hardly varies, even though ε varies over two orders of magnitude. This can also be seen in Figure 9, which shows the boundaries of the intrusion depicted in Figures 3-7, on the one diagram.

5. ASYMPTOTIC SOLUTIONS FOR THE FAR FIELD

The computation of the flow in the intrusion downstream from the source region is potentially complex, because it requires the description of the external flow, which becomes three-dimensional when $D \leq O(\varepsilon)$. However, an analysis of the asymptotic properties far downstream (for large R), of a thin intrusion spreading in uniform flow, is possible. This has been done for two situations: firstly, for inviscid flow, and secondly, and more realistically, incorporating the effect of drag of the environmental fluid on the intrusion. In both cases, we have

$$\int_0^{\theta_m(R)} RDU \mathrm{d}\theta = \frac{\pi}{2} , \qquad (16)$$

where $\theta_m(R)$ is the maximum value of θ for given R, on the boundary. On this boundary, we also have the spreading condition for an intrusive gravity current, which must here spread in the presence of ambient flow (Simpson 1997):

$$A_1 D(R,\theta_m) = \varepsilon \sin\theta_m , \qquad (17)$$

where A_1 is a proportionality factor of order unity.

In the inviscid case, $U \sim (1+\varepsilon^2)^{1/2}$, and in the drag-affected case it is $U_c \sim \varepsilon$ (where subscript "c" denotes a Cartesian velocity). Hence, since U is finite and R large it follows that D and θ_m must be small. In consequence we obtain

$$D \cong \left[\frac{\varepsilon\pi}{2A_1U_a}\right]^{1/2} \frac{1}{R^{1/2}}, \theta_m = \left[\frac{A_1\pi}{2\varepsilon U_a}\right]^{1/2} \cdot \frac{1}{R^{1/2}}, \qquad (18)$$

where U_a denotes the asymptotic velocity (in either the R- or X-directions), which equals $(1+\varepsilon^2)^{1/2}$ for the inviscid case, and ε for the realistic case with drag of the environment, which forces the intrusion to have the same mean velocity, to leading order.

These results imply that the width of the intrusion at large R, denoted Y_m, increases as $R^{1/2}$ (or $X^{1/2}$), for R (or X) large. Hence, the intrusion continuously expands with distance from the source. This is shown graphically in Figure 10.

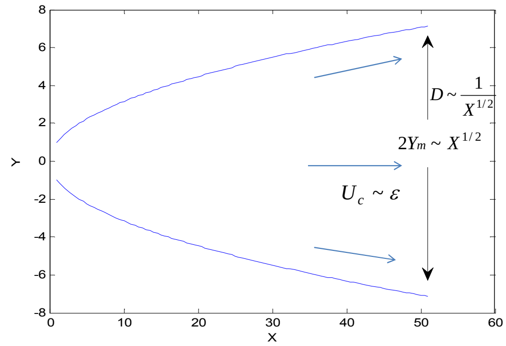

Figure 10. Asymptotic form of the intrusion for large distances from the source, for the case with turbulent drag from the environment.

References.

Akar, P. and Jirka, G.H. 1995a Buoyant spreading processes in pollutant transport and mixing. Part 1: Lateral spreading with ambient current advection. *J. Hydraulic Res*. **32**, 815-831.

Akar, P. and Jirka, G.H. 1995b Buoyant spreading processes in pollutant transport and mixing. Part 2: Upstream spreading in weak ambient current. *J. Hydraulic Res*. **33**, 87-100.

Baines, P.G. 1995 *Topographic Effects in Stratified Flows.* Cambridge University Press, 482 pp.

Baines. P.G., Jones, M.T. and Sparks, R.S.J. 2008 The variation of large-magnitude volcanic ash cloud formation. *J. Geophys. Res.* 113, D21204, doi:10.1029/2007JD009568.

Milne-Thomson L.M. 1960 *Theoretical Hydrodynamics*, MacMillan.

Simpson, J.E. 1997 *Gravity Currents*, 2nd edition. Cambridge University Press, 244 pp.